JOURNAL OF APPLIED ELECTROCHEMISTRY 17 (1987) 574–582

Electrodeposition of zinc–nickel alloys from chloride solution

L. FELLONI, R. FRATESI, E. QUADRINI, G. ROVENTI

Dipartimento di Scienze dei Materiali e della Terra, Facoltà di Ingegneria, Università di Ancona, Italy

Received 24 February 1986; revised 1 June 1986

Operating conditions for zinc and nickel codeposition from chloride baths were studied in order to obtain alloys containing up to 20% nickel. Satisfactory deposits were produced at 50°C using current densities ranging from 5 to 20 mA cm^{-2} and nickel to zinc ratios ranging from 6.8 to 37.5%.

Under the conditions studied, an empirical relationship was deduced in order to calculate the nickel percentage in the deposit from baths of prefixed composition using a given current density. Deposits having a nickel concentration lower than 11% were found to comprise the δ and γ phases, while at higher nickel concentration (up to 20%), the alloys showed only the γ phase structure, with preferred orientation (4 4 2) and (6 0 0) and excellent microhardness and corrosion resistance properties.

1. Introduction

Improved corrosion resistance requirements, production costs and pollution problems have led researchers and producers to study and develop processes for steel protection using multilayer electrogalvanized coatings [1–3], composite zinc films [4–7] and, especially, alloy zinc plating [8–15]. These processes are of particular interest to the auto-industry where precoated steel panels must satisfy many parameters, such as formability, weldability, paint adhesion properties and so on. At present, some of these parameters with hot dip galvanized sheets and conventional zinc electroplating are inadequate or insufficient.

Increasing interest has been directed towards zinc–iron [7, 9] and, especially, zinc–nickel [10–15] alloy coatings that appear to be particularly attractive since, under suitable electroplating conditions, these deposits exhibit better physical and electrochemical properties than a pure zinc layer. Most of the recent papers cited in the scientific and marketing literature dealing with improved zinc electroplating report studies and applications performed by Japanese authors. Many papers are concerned with patents and therefore little information on the bath compositions is given.

Shibuya and co-workers [10, 11] describe in some detail the considerable interdependence existing between process variables such as Ni^{2+}/Zn^{2+} mole ratio in the sulphate electrolyte, temperature, flux rate of electrolyte, current density on one hand and, on the other, chemical and physical properties of electrodeposits such as chemical composition, crystalline structure, weldability, flaking properties and corrosion resistance. These authors point out that, as in the case of plated steel sheets produced by an industrial electrogalvanizing line, the best behaviour is exhibited by a zinc–nickel alloy electrodeposit containing about 13% nickel and consisting wholly of the γ phase.

Raman *et al.* [13] have developed a sulphate bath for the deposition of bright zinc–nickel alloys which is proposed as a satisfactory substitute for cadmium coating. This type of bath, as well as that used by Shibuya [10, 11] can operate with higher nickel concentrations than zinc, rather low pH values (pH range 2 to 3) and at high current densities.

In a recent review, Hall [14] emphasized that zinc–nickel alloy deposits are generally of the

0021–891X/87 $03.00 + .12

anomalous type according to the definition of Brenner [16]. Moreover, Hall pointed out that: (i) there are important differences between the phase limits observed in deposits electrochemically produced and those of thermally prepared zinc–nickel alloys; (ii) the β' phase has never been identified in electrodeposits; (iii) the γ phase, identified in deposits containing 12–14% nickel, provides the best corrosion resistance. The excellent performance of zinc–nickel alloy deposits containing 6–20% nickel, obtained by non-cyanide chloride baths by means of the Boeing process, is described by Hsu [15] who points out the fundamental necessity to produce coatings that have very low hydrogen embrittlement properties. For this reason it is clear that the electroplating conditions must be chosen in order to limit hydrogen ion reduction during electrolysis and to exclude any poison of the hydrogen recombination reaction. On the other hand, it is known that baths that operate at pH values near neutral are not suitable because at pH 5–6 zinc and nickel hydroxide formation is appreciable [17]. Indeed, Hall [14] reports that inclusions of $ZnSO_4 \cdot 3Zn(OH)_2 \cdot 4H_2O$ and possibly NiO and $NaNiO_2$ have been identified by Dini and Johnson [18] by means of X-ray diffraction analysis of zinc–nickel alloys deposited from a mixed sulphate–sulphamate bath at pH 5.

No pertinent data are available for a comparison between the behaviour of deposits with and without inclusions, but it appears logical to suppose that such inclusions worsen the coating properties. In any case, there is today a tendency to prefer single phase zinc–nickel alloy deposits and, particularly in industrial zinc plating lines, to use chloride solutions. Indeed, chloride baths are considered to be advantageous [19] in that they allow for satisfactory plating of malleable iron castings and any barrelled tools or devices.

Most of the papers dealing with chloride baths are concerned primarily with electrodeposits of commercially acceptable quality, or with industrial application in continuous production lines of coated steel sheets. Therefore, little information is available on detailed operating conditions with solutions of low nickel concentrations.

In the present work, zinc–nickel alloy electrodeposits were obtained on iron from a chloride bath with various concentrations of nickel in order to relate the percentage of nickel in the electrodeposit with: (i) the percentage of nickel existing in the solution; (ii) the presence of different phases in the deposit; (iii) the microhardness of the electroplate; and (iv) the salt-spray test resistance.

In addition, the effect of both the current density and the temperature on the nickel content in the electrodeposited zinc–nickel alloy was investigated.

2. Experimental details

Electrodepositions were carried out under galvanostatic conditions at 5, 10, 15 and 20 mA cm^{-2}. A three-compartment plexiglass cell was used. The central cathodic compartment was joined to the two lateral anodic compartments by a porous membrane which prevented the diffusion of anodic products to the cathodic compartment during electrolysis.

The cathodic solution (0.5 dm^3) and both the anodic solutions (total volume 0.5 dm^3) were changed after six to eight electrodepositions. Electrodeposits were obtained on both sides of ARMCO iron discs, 1 mm thick (exposed area 15 cm^2), which were vertically positioned at equal distance from the porous membranes. The two pure zinc anodes had a total exposed area of 50 cm^2.

Before immersion, the iron surfaces were ground with wet 1000 grade SiC emery paper, washed in distilled water and ethanol and dried with hot air. The polarization at each prefixed current density was applied at immersion and the electrolysis was continued until deposits, 6–12 μm thick, were obtained. The cathodic solution was lightly agitated by a glass stirrer. For each electrodeposition condition at least three separate tests were carried out.

Pure zinc deposits were obtained at 25°C using the following solution: 70 g dm^{-3} $ZnCl_2$ (0.51 M Zn^{+2}), 26 g dm^{-3} H_3BO_3, 220 g dm^{-3} KCl, 30 ml dm^{-3} ethoxylate of fatty acids, at 20 mA cm^{-2} and pH 5.5. Zinc–nickel alloy electrodepositions were obtained at 50° C using baths of the following composition: 236 to 147 g dm^{-3} $ZnCl_2$ (1.73 to 1.08 M Zn^{2+}) 34 to 123 g dm^{-3}

$NiCl_2 \cdot 6H_2O$ (0.14 to 0.53 M Ni^{2+}), 40 g dm^{-3} H_3BO_3, 0.16 g dm^{-3} hexylsulphate at pH 3.5–4. Solutions were prepared with doubly distilled water and analytical grade reagents.

Concentrations of $ZnCl_2$ and $NiCl_2 \cdot 6H_2O$ were varied in such a manner that the total salt content in the baths ranged from 1.87 to 1.60 M. The percentage of nickel present in the baths and the deposit, indicated by Ni_{sol} and Ni_{dep}, respectively, was calculated as proposed by Brenner [16]:

$$\%\,Ni = 100\left[\frac{\text{mass Ni}}{\text{total mass (Ni + Zn)}}\right]$$

After plating, the disc cathodes were thoroughly washed with water and then ethanol, hot air dried and weighed.

To determine the percentage composition of the electrodeposited alloys the deposits were stripped in a minimum volume of 1 : 3 HCl solution and analysed for nickel and zinc by means of Inductively Coupled Plasma spectroscopy (ICP Perkin–Elmer 5005 model). The morphology of the deposits was observed by means of scanning electron microscopy (SEM). The deposited phases were analysed by the X-ray diffraction method by CuKα (λ = 1.54 Å) and identified by Powder Diffraction File card (JCPDS). The Knoop microhardness of deposits, 12 μm thick, was measured using 5 to 25 g loads in order to obtain an indentation depth lower than 1/10 of the deposit thickness.

To investigate the influence of temperature on the deposit characteristics, electrodepositions were carried out at 40 and 60°C.

3. Results and discussion

3.1. *Effect of operating variables on percentage of nickel in the deposits*

The operating conditions used were chosen, after numerous preliminary tests, in order to obtain reproducible zinc–nickel deposits with satisfactory physical and chemical properties using chloride baths with cathodic current efficiencies higher than 97%.

Cathodic current densities of 5 to 25 mA cm^{-2} were used, since lower values have no practical application while higher values yielded non-

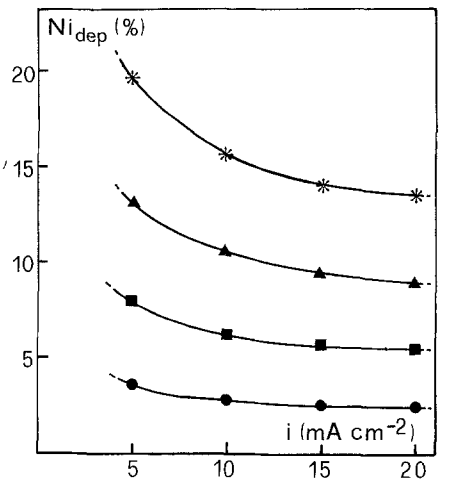

Fig. 1. Effect of current density on the percentage of nickel (Ni_{dep}) in zinc–nickel alloys electrodeposited from baths containing the following percentage of nickel (Ni_{sol}): *, 37.5%; ▲, 25%; ■, 15%; ●, 6.8%.

homogeneous deposits due to co-evolution of hydrogen. The effect of current density on the percentage of nickel in the zinc–nickel alloys electrodeposited from baths containing various percentage of nickel is shown in Fig. 1. Under the operating conditions used, the content of nickel in the deposit can be calculated by the following empirical relationship:

$$Ni_{dep} = \left(\frac{1.37 + 0.30i}{i}\right) Ni_{sol}$$

where i is the total electrolysis current density in mA cm^{-2}.

This relationship is valid for Ni_{sol} ranging from 5 to 40%. Analogous relationships have been found for plating processes previously studied [20, 21].

The percentage of nickel in the electrodeposited zinc–nickel alloys with respect to the percentage of nickel in the plating bath at various current densities is given in Fig. 2. The position of the curves in this figure with respect to the composition reference line (CRL), shows that, under the electrolysis conditions used, zinc is the more readily deposited metal and the nickel deposition is, according to Brenner [16], of anomalous type. Normal codeposition, i.e. preferential or equilibrium electroreduction of the more noble metal, would show curves lying

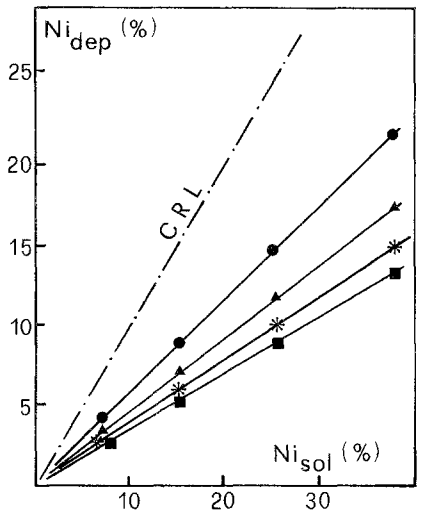

Fig. 2. Percentage of nickel in electrodeposited zinc–nickel alloys versus percentage of nickel in the baths at the following current densities (see text for base-bath composition): ●, 5 mA cm^{-2}; ▲, 10 mA cm^{-2}; ∗, 15 mA cm^{-2}; ■, 20 mA cm^{-2}.

above the CRL. For normal codeposition two essential conditions must be satisfied: (i) the ionic concentration of the more noble metal in the plating bath should be such as to allow its cathodic reaction to take place according to the Nernst relationship at the potential value which is established by the total electrolysis current density; (ii) kinetic parameters of the more noble metal reduction process should be favourable.

Even if the concentration ratio of the more noble metal to zinc is suitable and the alloy plating is not under diffusion control, it is known that most electrodepositions of alloys containing zinc and an iron-group metal are anomalous when the current density is higher than a critical value. According to Hall [14], the explanation suggested by Higashi *et al.* [7] for zinc–cobalt codeposition may be regarded to be valid for all these 'anomalous' electrodepositions and, consequently, also for zinc–nickel alloy deposition. Higashi *et al.* [7] believe that at higher current densities a local pH increase at the cathodic surface causes the formation of zinc hydroxide. This film of zinc hydroxide acts as a physical barrier to the reduction process of the more noble metal.

In our opinion such an explanation is sound only in particular plating conditions which produce an unsatisfactory zinc–nickel alloy, probably containing hydroxides. Usually a buffer is added to a plating bath to limit pH variations at the cathodic surface and to prevent precipitation of hydroxides. The most likely explanation for the anomalous codeposition is that the kinetic cathodic reaction parameters of the iron-group metals are so unfavourable that they destroy the thermodynamic nobleness of these metals with respect to zinc.

According to Piontelli's [22] definition these metals are known to be electrochemically inert for ionic exchange reactions. They are, generally, characterized by very low exchange current densities, unlike zinc which shows high exchange current density. The values of this important kinetic parameter depend on the solution composition, but at present only data for simple systems are available (Table 1). Considerable differences in the values of the exchange current densities of nickel and zinc are also likely to exist in more complex solutions. In addition, in accordance with Foerster [26], the overpotential for the deposition of the transition metals is increased by the codeposition of zinc. Accordingly, a negative cathode potential is reached at which the deposition of a high-zinc alloy is permitted.

Comparative overpotential measurements of nickel deposition from chloride solutions on

Table 1. Exchange current densities for Zn^{2+}/Zn and Ni^{2+}/Ni equilibria in different solutions

Metal	*Solutions*	i_0 *(A cm^{-2})*	*Reference*
Nickel	2 N KCl + 0.01 N $NiCl_2$ (pH = 5.96)	1×10^{-8}	[23]
Nickel	Sulphate	2×10^{-9}	[24, 25]
Zinc	Chloride	3×10^{-4}; 7×10^{-1}	[24, 25]
Zinc	Sulphate	3×10^{-5}	[24, 25]

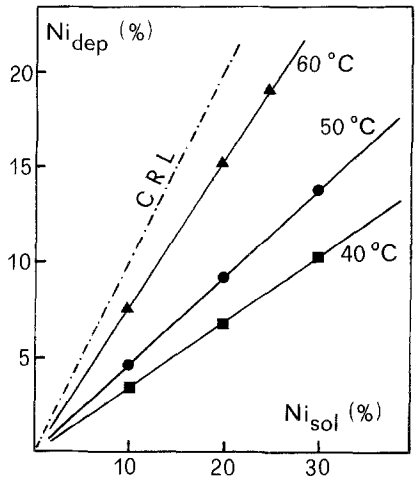

Fig. 3. Effect of temperature on the nickel content in zinc–nickel alloys electrodeposited from baths containing various percentages of nickel. Current density, 10 mA cm^{-2}.

cathodes of pure nickel and zinc–nickel alloy will be carried out in the future.

It is evident from Fig. 3 that the percentage of deposited nickel, at prefixed current density, increases significantly with rising temperature for any studied nickel content in the plating bath. This fact supports the above assumption concerning the important role played by temperature-dependent kinetic parameters.

3.2. *Appearance and microstructure of the electrodeposits*

The deposits of pure zinc appeared bright yellowish-grey, while the appearance of the electrodeposited zinc–nickel alloys depended on the nickel content: at lower nickel percentage dull silver-grey deposits were observed, but with an increased nickel content the deposits showed a greater brightness, particularly those obtained at lower current densities. The structure of the deposits observed by means of SEM changed clearly with the codeposition of nickel, as shown in Figs 4–8. Pure zinc had a granular appearance, whereas a 3.5% nickel content produced an irregular distribution of pyramidal crystallites. When the percentage of nickel increased, these crystallites progressively coated almost the entire plated surface and clearly showed a preferred orientation. At higher nickel content, regardless of current density used, fine-grained pyramidal crystallites were observed. X-ray diffraction analysis results suggest that such crys-

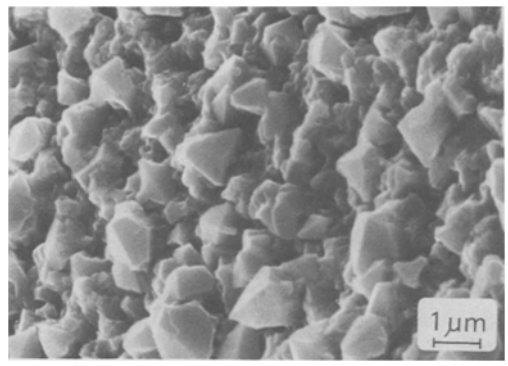

Fig. 5. Electrodeposited zinc–nickel alloy with 3.5% nickel. Current density, 10 mA cm^{-2}.

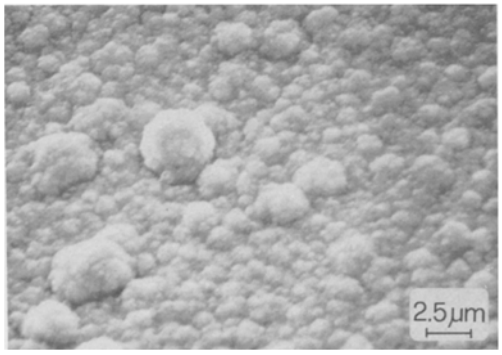

Fig. 4. Pure zinc electrodeposit. Conditions reported in Experimental section.

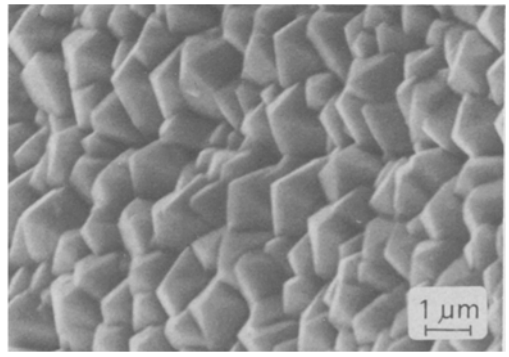

Fig. 6. Electrodeposited zinc–nickel alloy with 8.5% nickel. Current density, 5 mA cm^{-2}.

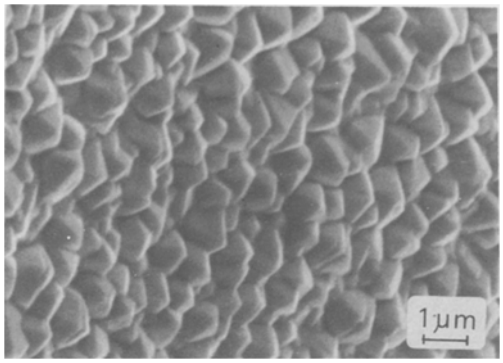

Fig. 7. Electrodeposited zinc–nickel alloy with 14.5% nickel. Current density, 5 mA cm^{-2}.

tallites are γ-phase as observed on the electrodeposited zinc–nickel alloy when the nickel content is above 11%.

The identification of the phases of the deposits was obtained from line profiles of the X-ray reflection plotted as a function of 2θ (Fig. 9). The value of the angles corresponding to the peaks found, the indexes of the crystallographic planes of the phases identified, as well as the average value of the lattice parameter of the phase are given in Table 2. Under the operating conditions used, the phases of the deposits were found to depend on the nickel content in the electrodeposited alloy but not on the current density in the range considered. Deposits containing 3.5 and 11.5% nickel were characterized by a two-phase (δ and γ) structure. The γ phase showed a preferential (3 3 0) and (4 1 1) orientation.

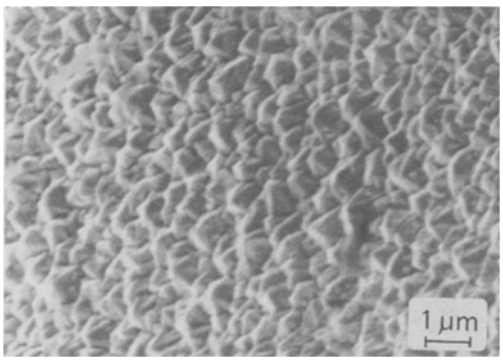

Fig. 8. Electrodeposited zinc–nickel alloy with 22.0% nickel. Current density, 5 mA cm^{-2}.

Table 2. Crystallographic orientation of zinc and zinc–nickel alloy by X-ray diffraction

Phase	h k l	2θ	a_0
	(3 2 1)	36.80°	
	(4 1 1) (3 3 0)	43.18°	
	(3 3 2)	47.80°	
γ	(4 4 2) (6 0 0)	62.70°	8.91
	(6 2 2)	70.60°	
	(4 4 4)	73.60°	
δ	(5 5 2)	78.59°	
	(0 0 4)	39.0°	
Zinc	(1 0 0)	39.10°	
	(1 0 1)	43.20°	
	(1 0 3)	70.25°	
	(1 1 2)	83.30°	

A higher reflection intensity (Fig. 9) corresponding to the (4 4 2) and (6 0 0) orientations of the γ phase resulted with increasing nickel percentage in the electrodeposits. The zinc–nickel alloys with 14.5 and 20% nickel were found to be formed of the single γ phase, which agrees with the zinc–nickel equilibrium diagram as already noted by some authors [11, 27, 28]. Shibuya

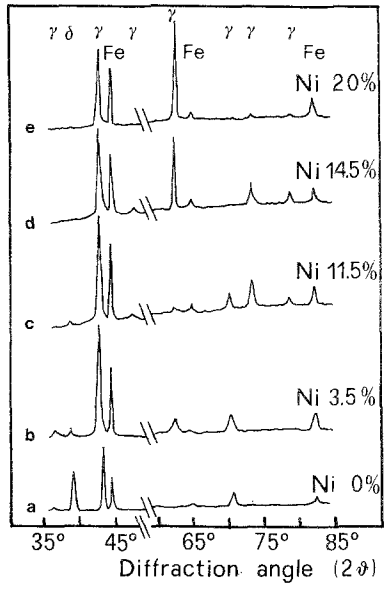

Fig. 9. X-ray diffraction of electrodeposits on iron (CuKα; λ = 1.54 Å). (a) Pure zinc; (b, c, d, e) zinc–nickel alloys.

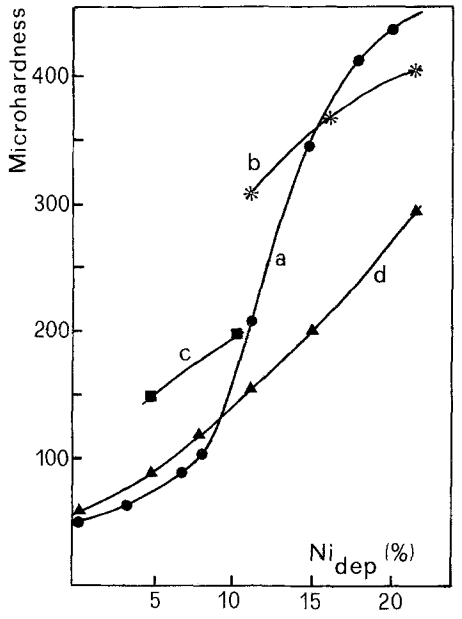

Fig. 10. Variation of microhardness versus the percentage of nickel in the deposit. (a) Present research: electrodeposits, 12 μm thick; load, 5–25 g. (b) Data from [13]; (c) data from [28]; (d) data from [29].

et al. [11], however, have always obtained deposits with preferred orientation (3 3 0) and (4 1 1), while in the present research, from 14.5 to 20% nickel, an increasing preferred orientation (4 4 2) and (6 0 0) was observed.

3.3. *Microhardness measurements*

The measured microhardness values of the electrodeposited zinc–nickel alloys are given in Fig. 10 where data obtained by other authors [13, 29, 30] for deposits produced under different operating conditions are also shown. The comparison shows clearly that the microhardness of the electrodeposited zinc–nickel alloy depends on both the nickel content and the bath composition as well as the processing variables. Moreover, the values obtained in the present research indicate that microhardness did not increase linearly with increasing nickel percentage, but a sharp increase was found in the range 8 to 10% nickel in the electrodeposits. This agrees with the structure modification observed with SEM in the same composition range and with the presence of the single γ phase,

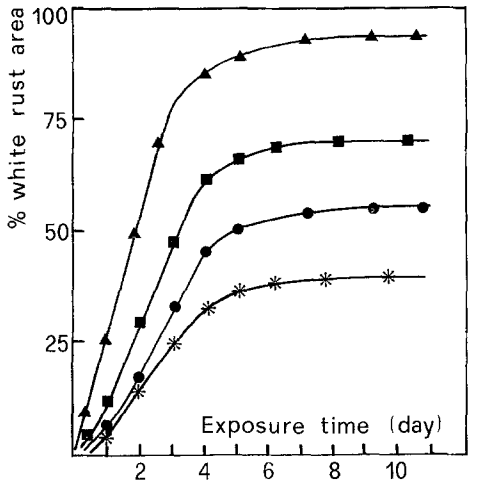

Fig. 11. Propagation of white rust on the pure zinc and zinc–nickel alloys electroplated on iron discs during the salt-spray test (5% NaCl at 35°C). Values of Ni_{dep}: ▲, 0%; ■, 8.5%; ●, 14.5%; *, 20%.

when the nickel content is above 11%, found by X-ray diffraction analysis.

3.4. *Corrosion resistance*

The corrosion resistance of the various electrodeposited zinc–nickel alloys was evaluated by observing the propagation of both white and red rust formed on coatings, 6 μm thick, which were

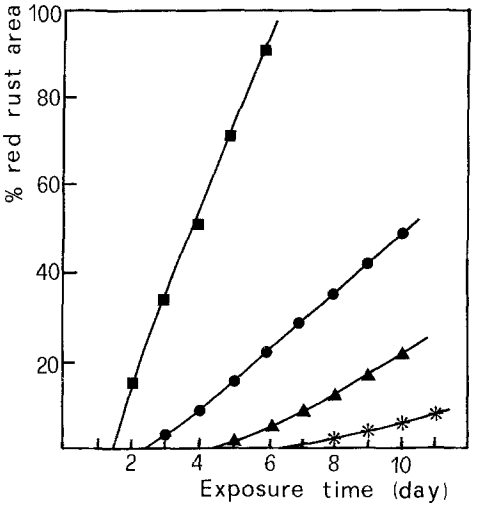

Fig. 12. Propagation rate of red rust on the pure zinc and zinc–nickel alloys electroplated on iron discs during the salt-spray test (5% NaCl at 35°C). Symbols for Ni_{dep} as for Fig. 11.

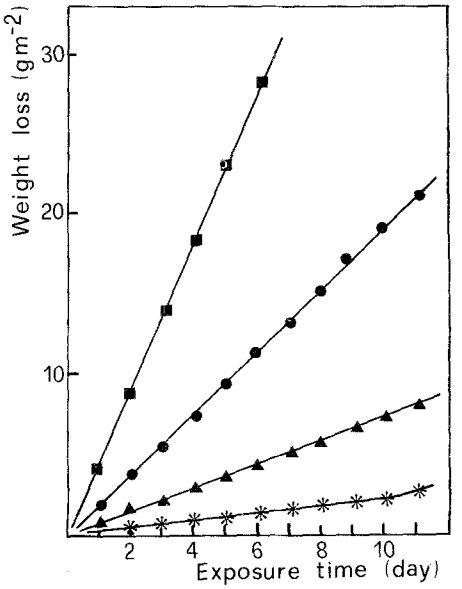

Fig. 13. Corrosion weight-loss of electrodeposited pure zinc and zinc–nickel alloys by the salt-spray test (5% NaCl at 35°C). Deposits of 43 $g\,m^{-2}$ (approximately 6 μm thick). Symbols for Ni_{dep} as for Fig. 11.

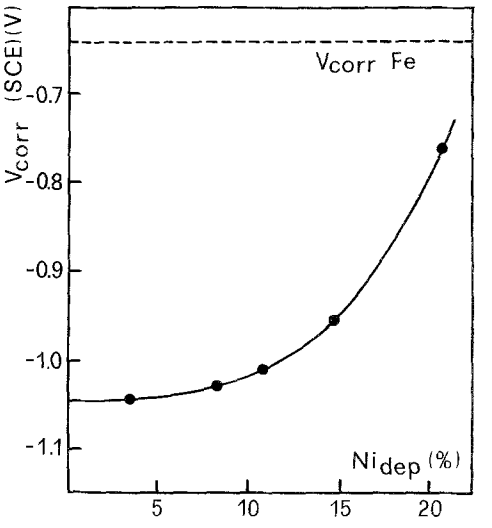

Fig. 14. Effect of the percentage of nickel in the deposit on the free corrosion potential of zinc–nickel electrodeposits after immersion in aerated 5% NaCl solution, at room temperature, for 30 min. V_{corr} of iron under the same conditions is −0.640 versus SCE.

tested in a 5% neutral salt-spray environment at 35°C. Results expressed as a percentage of the surface coated by either white or red rust as a function of the exposure time are illustrated in Figs 11 and 12, respectively. The appearance time of white rust depended very little on the nickel content of the deposit. However, the percentage of the surface coated by white rust was found to be lower with increasing nickel fraction and to remain constant after about 120–140 h exposure. The occurrence of red rust appeared to be dependent on the percentage of nickel of the deposits. Red rust spread at a constant rate up to about 300 h exposure.

Weight losses of electroplated specimens as a function of exposure time in the salt spray (Fig. 13) show that the corrosion resistance of the zinc–nickel deposits improved when the nickel percentage of the alloy was increased in all the composition ranges studied.

Free corrosion potential values measured after 30 min of immersion in aerated 5% NaCl solution are given in Fig. 14. The potentials of all the zinc–nickel alloys studied were more negative than that of ARMCO iron under the same conditions. It is evident, therefore, that such electrodeposits can give cathodic protection to the iron base. Moreover, since the difference in the potentials of the iron and the zinc–nickel alloy is rather small, during cathodic protection action the latter will corrode slowly and thus the life of any object will increase.

4. Conclusion

The results obtained in the present research demonstrate the improved performance of zinc–nickel alloy deposits compared with zinc electroplating, particularly those deposits containing a nickel fraction above 11%. This is due to the fact that the electrodeposited alloy has a single γ-phase structure above this percentage.

However, a precise comparison between the present corrosion resistance results and those of other authors is not possible due to the differences in the testing conditions and, above all, in the thickness and structure of the electrodeposits. These differences are such as to make any assessment of suitability of the various baths and the operating conditions used by other laboratories inconclusive.

References

[1] A. Catanzaro, G. Arrigoni, M. Palladino and M. Sarracino, SAE Tech. Pap. Series, No. 830583, Detroit, Michigan (1983).

[2] M. Memmi, R. Bruno and M. Palladino, *Mater. Perform.* **2** (1983) 9.

[3] S. Kado, S. A. Yusawa and T. Watanabe, *Tetsu to Hagane* **66** (1980) 790.

[4] T. Adaniya, *Sheet Metal Ind. Int.* **12** (1978) 73.

[5] K. Ariga and K. Kanda, *Tetsu to Hagane* **66** (1980) 797.

[6] T. Adaniya, M. Omura, K. Matsudo and H. Naemura, *Plat. Surf. Finish.* **68** (1981) 96.

[7] K. Higashi, H. Fukoshima, T. Urokawa, T. Adaniya and K. Matsudo, *J. Electrochem. Soc.* **128** (1981) 2081.

[8] T. Fukuzuka, K. Jajiawara and K. Miki, *Tetsu to Hagane* **66** (1980) 807.

[9] T. Watanabe, M. Omura, T. Honma and T. Adaniya, SAE Tech. Pap. Series, No. 820424, Detroit, Michigan (1982).

[10] A. Shibuya, T. Kurimoto, K. Korekawa and K. Noji, *Tetsu to Hagane* **66** (1980) 771.

[11] R. Noumi, H. Nagasaki, Y. Foboh and A. Shibuya, SAE Tech. Pap. Series, No. 820332, Detroit, Michigan (1982).

[12] T. Kurimoto, Y. Hoboh, H. Oishi, K. Yanagawa and R. Noumi, SAE Tech. Pap. Series, No. 831837, Detroit, Michigan (1983).

[13] V. Raman, M. Pushpavanam, S. Jayakrishnan and B. A. Shenoi, *Met. Finish.* **81** (1983) 85.

[14] D. E. Hall, *Plat. Surf. Finish.* **71** (1983) 59.

[15] G. F. Hsu, *ibid.* **71** (1984) 52.

[16] A. Brenner, 'Electrodeposition of Alloys', Vols I and II, Academic Press, New York and London (1963).

[17] M. Pourbaix, 'Atlas of Electrochemical Equilibria in Aqueous Solutions', NACE, Houston, Texas (1974) p. 406.

[18] J. W. Dini and H. R. Johnson, Sandia Lab. Report 77-8511, 'Electrodeposition of Zinc–Nickel Alloy Coatings' (Oct. 1977).

[19] T. Sharretts, *Prod. Finish.* **47** (1982) 66.

[20] R. Fratesi and G. Roventi, *La Metall. Ital.* **5** (1983) 339.

[21] R. Fratesi, G. Roventi, M. Maja and N. Penazzi, *J. Appl. Electrochem.* **14** (1984) 505.

[22] R. Piontelli, in 'Atlas of Electrochemical Equilibria in Aqueous Solutions' (edited by M. Pourbaix), NACE, Houston, Texas (1974) 11.

[23] A. J. Bard, 'Encyclopedia of Electrochemistry of the Elements', Vol. 3, Marcel Dekker, New York (1975) p. 282.

[24] J. M. West, 'Electrodeposition and Corrosion Processes', Van Nostrand Reinhold (1970).

[25] *Idem*, in 'Corrosion', Vol. II, 2nd edn (edited by L. L. Shreir), Newnes-Butterworths (1976) pp. 21, 38.

[26] F. Foerster, 'Elektrochemic Wosseriger. Lösungen' 4th edn, Barth, Leipzig (1923).

[27] T. L. Rama Char and S. K. Panikkar, *Electroplat. Met. Finish.* **13** (1960) 405.

[28] M. R. Lambert, R. G. Hart and H. E. Townsend, SAE Tech. Pap. Series, No. 831817, Detroit, Michigan (1983).

[29] H. Tsuji and M. Kamitani, Proc. AES 69th Annual Conference, paper P2 (20–24 June, 1982).

[30] S. R. Rajagopalan, *Met. Finish.* **70** (1972) 52.